

Evaporation-based microfluidic production of oil-free cell-containing hydrogel particles

Rong Fan,¹ Kubra Naqvi,² Krishna Patel,³ Jun Sun,⁴ and Jiandi Wan^{1,a)}

¹Microsystems Engineering, Rochester Institute of Technology, Rochester, New York 14623, USA

²College of Science, Rochester Institute of Technology, Rochester, New York 14623, USA

³Webster Schroeder High School, Webster, New York 14580, USA

⁴Department of Biochemistry, Rush University, Chicago, Illinois 60612, USA

(Received 19 December 2014; accepted 27 February 2015; published online 27 March 2015)

We demonstrate an evaporation-based microfluidic strategy to produce oil-free cell containing hydrogel particles. Perfluoro-*n*-pentane, which is used as the continuous oil phase to generate cell-containing hydrogel (Extracel) particles, is removed at an elevated temperature. Human colon cancer cells (HCT116) encapsulated in the hydrogel particles show higher viability than cells encapsulated in particles that are produced via a non-evaporative oil phase. In addition, single HCT116 cells can be cultured for a week in such particles and respond to inflammatory stimuli, highlighting the potential applications of the developed strategy for 3D cell culture, drug testing, and cell-based drug delivery. © 2015 AIP Publishing LLC.

[<http://dx.doi.org/10.1063/1.4916508>]

INTRODUCTION

Cells cultured in a three-dimensional (3D) hydrogel matrix resemble and simulate various functions of real tissue, and have drawn significant attentions in the fields of tissue engineering,¹ stem cell research,² drug screening,³ and cell-based drug delivery.⁴ In particular, because micrometer diameter hydrogel particles provide a well-controlled, physically isolated microenvironment for 3D cell culture,^{5,6} numerous methods including extrusion,⁷ complex coacervation,⁸ emulsification,⁹ and microfluidics¹⁰ have been developed to encapsulate cells in hydrogel particles. Recent advances in microfluidics, in particular, have yielded unprecedented control over the generation of hierarchical emulsion drops and hydrogel particles,^{11–13} and thus have significantly improved the efficiency of cell microencapsulation. Microfluidic generation of cell-containing aqueous drops and/or particles, however, usually occurs in a continuous oil phase, which unavoidably results in oil contamination of particles and cells. Because oil contamination is toxic and has showed to be able to inhibit cell growth, accelerate cell death, and damage the formation of tissue,^{14,15} microfluidic approaches that are able to produce oil-free cell-containing particles are of great interest.

Colorectal cancer cells, on the other hand, have been cultured in 3D matrixes to recapitulate the *in vivo* structure of colon tumors.¹⁶ These 3D culture systems have been used for testing anti-cancer drugs^{17–19} and to address functional interactions among colorectal cancer cells, stromal cells, and the extracellular matrix.^{20,21} Particularly, it has been shown that 3D culture environment impacts the activities of colorectal cancer cells including morphologic types, proliferation, and gene expression. The majority of studies of colorectal cancer cells in 3D matrixes, however, are conducted under a bulk 3D culture environment, where hundreds of colon cancer cells are cultured together in a matrix. As a result, cell-to-cell communications likely affect the activities of colorectal cancer cells, compromising the impact of 3D environment on cellular activities. Studies of 3D-growth of single cancer cells in a physically isolated microenvironment *per se*, however, are limited.

^{a)} Author to whom correspondence should be addressed. Electronic mail: jdween@rit.edu. Telephone: 585-475-7726.

Here, we demonstrate a microfluidic approach to produce oil-free hydrogel particles with controlled numbers of encapsulated human HCT116 colon cancer cells and investigate the growth of single HCT116 cells in a physically isolated 3D microenvironment. To produce oil-free hydrogel particles, we utilize perfluoro-*n*-pentane (PFP) as the continuous oil phase to generate aqueous cell-containing droplets. Because PFP has a boiling point of 29 °C, it can be removed effectively by evaporating the oil phase at 37 °C. Meanwhile, Extracel hydrogel precursors, which are widely used for cell culture including colon cancer cells,²² are added to the aqueous cell-containing droplets and become gelation at 37 °C. As a result, oil-free hydrogel particles can be generated by simultaneously evaporating the PFP oil phase and solidifying the hydrogel precursor-containing aqueous drops at 37 °C. Furthermore, we show that when HCT116 cells are encapsulated in the oil-free hydrogel particles, HCT116 cells show a higher viability than that encapsulated in particles generated via conventional approaches. In addition, we find that, at the single cell level, encapsulated HCT116 cells grow slower and are more susceptible to inflammatory stimuli than cells cultured in petri dish, highlighting the regulatory role of the confined 3D microenvironment for cell proliferation and homeostasis. To the best of our knowledge, this is the first demonstration of an evaporation-based microfluidic approach to produce oil-free cell-containing hydrogel particles and the investigation of 3D-culture of single colorectal cancer cells in a physically isolated microenvironment.

MATERIALS AND METHODS

Cell culture and maintenance, microfluidic generation of drops, and encapsulation of HCT116 human colon cancer cells in drops are described in detail in the supplementary material.³⁵ To generate Extracel hydrogel particles with encapsulated HCT116 cells, a HyStem-C Hydrogel Kit (BD Biosciences) was utilized as the Extracel hydrogel precursors, which consisted of Glycosil (thiol-modified sodium hyaluronate), Gelin-S (thiol-modified gelatin), Extralink (PEGDA, polyethylene glycol diacrylate), and degassed, deionized (DI) water. The Glycosil and Gelin-S powder were dissolved in 1 ml DI water separately and Extralink powder was dissolved in 0.5 ml DI water. The cell-monomer mixture was prepared by well mixing 150 μ l Glycosil and 150 μ l Gelin-S in a 1 ml centrifuge tube, followed by adding 150 μ l HCT116 cell solution (1×10^8 cells ml^{-1}). Oil as continuous phase was prepared by adding 2 wt. % PEG-157 surfactant, which is synthesized based on the previous report,²³ into perfluoro-*n*-pentane (Strem Chemicals). 7500 Engineered Fluid (3MTM NovecTM) (HFE 7500) was prepared by adding 2 wt. % amine-modified Krytox. To evaporate the oil phase, cell encapsulating droplets with excess oil were collected in a 1 ml centrifuge tube and then incubated at 37 °C. The tube was taken out and weighed every 5 min to monitor the weight change.

RESULTS AND DISCUSSION

To control the generation of Extracel hydrogel particles, we have developed a flow-focusing microfluidic device that has two individual inlets to prevent hydrogel precursors from gelation during the process of sample introduction (Figure 1(a)). One of the inlets is for hydrogel monomers (Glycosil and Gelin-S) and the other inlet is for the crosslinker (Extralink). The crosslinker solution and hydrogel monomers mixed with a HCT116 cell suspension (1×10^8 cells ml^{-1}) are injected, respectively, into the two separated inlet channels, flowing through the confluence area and form droplets downstream in a continuous oil phase. To optimize the encapsulation efficiency for 2–4 cells per drops, we estimate the diameter of drops to be 50 μ m for a concentration of cells in the aqueous phase of 1×10^8 cells ml^{-1} , based on Poisson distribution equation (see supplementary material³⁵ for Figure S1).^{24,25} Indeed, when a typical aqueous flow rate of 4 μ l min^{-1} (for both aqueous phases) and oil flow rate of 40 μ l min^{-1} are used, we are able to generate cell-containing aqueous drops with an average diameter of 50 μ m. As shown in Figure 1(b) inset, the diameters of the majority of particles (>70%) fall into the range of 46–54 μ m. Only 6% and 5% of the particles have the diameters in the range of 30–38 μ m and 54–62 μ m, respectively. Cells encapsulated in drops are clearly evident in Figure 1(b). The percentage of droplets with two cells is 65% among all the cell-containing drops.

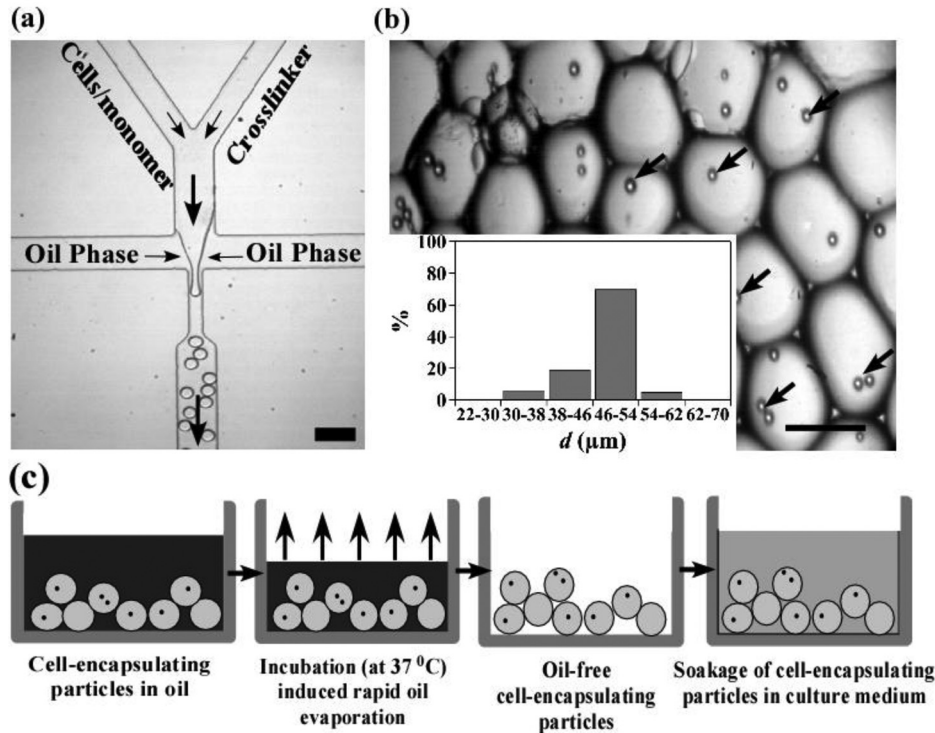


FIG. 1. Microfluidic encapsulation of HCT116 colon cancer cells in Extracel hydrogel particles. (a) Experimental image of a flow-focusing microfluidic device used to encapsulate cells in Extracel hydrogel particles (scale bar = 100 μm). Arrows indicate the direction of flow. (b) Image of hydrogel particles with encapsulated cells. Arrows indicate the encapsulated cells in particles (scale bar = 50 μm). Inset: size distribution of particles (calculated from more than 100 particles). (c) Schematics of the rapid oil removal process and cell culture in hydrogel particles.

To remove the PFP oil phase by evaporation, we collect the cell-containing drops in a 1 ml centrifuge tube and incubate the mixture solution at 37 $^{\circ}\text{C}$. The progress of evaporation is monitored by measuring the weight of the mixture solution at different incubation time (Figure 1(c)). For comparison, we also generate cell-containing drops in a HFE 7500 oil phase. The results show that the weight of the PFP mixture stops decreasing after incubating at 37 $^{\circ}\text{C}$ for 35–40 min, suggesting that the oil phase is evaporated completely (Figure 2(a)). In contrast, the removal of the HFE 7500 solution via evaporation is ineffective and the weight of HFE 7500 solution remains almost constant within 40 min. For a long time incubation, the weight of HFE 7500 solution decreases slowly over 1200 min (see the supplementary material³⁵ for Figure S2). Note that separation of the oil phase from particles by using conventional approaches such as centrifugation and filtration is not effective (see the supplementary material³⁵ for Figure S3). Rapid evaporation of PFP, however, results in an aggregation of cell-containing particles (Figure 2(a), inset). To prevent particles from aggregation, we collect the cell-containing drops in a centrifuge tube that is prefilled with a DMEM culture medium. As shown in Figure 2(b) inset, PFP from the continuous oil phase remains at the bottom of the centrifuge tube and the cell-containing drops form a layer between the culture medium and PFP. After the mixture is incubated for about 90 min, the weight of the mixture stops decreasing (Figure 2(b)), and particles are obtained without any aggregation in the DMEM culture medium.

We then study the cell viability by culturing the cell-containing particles at 37 $^{\circ}\text{C}$ in the DMEM medium, where nutrients in the medium are expected to be delivered to cells through diffusion. Our results show that the majority of cells (>90%) survive in the first 72 h, but the percentage of living cells shows a descending trend within the next 144 h (Figure 2(c)). In contrast, when HFE 7500 is used as the oil phase to generate cell-containing hydrogel particles, the percentage of living cells starts to decrease sharply after 24 h and drops to 0% within 120 h.

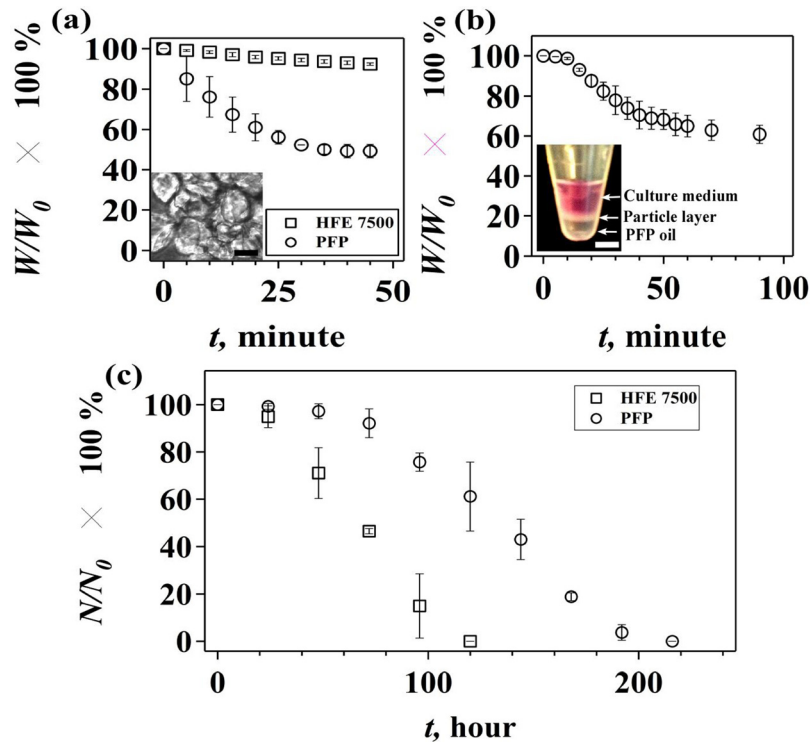


FIG. 2. Effect of oil on particle aggregation and cell viability. (a) Evaporation-induced change of weight percentage ($W/W_0 \times 100\%$) of the mixture solution of droplets and oil. W_0 is the weight of the mixture at $t=0$ min, and W is the weight at $t=n$ min ($n=5, 10, 15, 20, 25, 30, 35, 40,$ and 45). Inset: image of aggregated hydrogel particles after the removal of PFP (scale bar = $50 \mu\text{m}$). (b) Evaporation-induced change of weight percentage ($W/W_0 \times 100\%$) with time, when particles are collected in the DMEM cell culture medium. Inset: image of a centrifuge tube containing layers of culture medium, particles, and PFP (scale bar = 5 mm). (c) Percentage of living cells in hydrogel particles ($N/N_0 \times 100\%$) at different culture time (t). N_0 is the number of living cells at $t=0$ h, and N is number of living cells at $t=n$ hours ($n=24, 48, 72, 96, 120, 144, 168, 192,$ and 216). Error bar is presented as standard deviations of the mean, which is calculated based on three sets of independent experiments.

Note that cell-containing hydrogel particles generated in HFE 7500 oil are collected via centrifugation and cultured under the same condition as cell-containing hydrogel particles generated in PFP. HFE 7500 has been used extensively as the continuous oil phase in microfluidic-based generation of droplets or micro-particles due to its inertness and ability to provide superior droplet stability.²⁶ Our results, however, demonstrate a toxic effect of the residue HFE 7500 oil on the growth of encapsulated colon cancer cells.

We further investigate the cell proliferation dynamics at the single cell level and find that the cells encapsulated in hydrogel particles have a prolonged cell cycle and a relatively low proliferation rate. Encapsulated cells spend 3 days to grow before reaching the division stage, and the division process normally takes about 2.5 h, which is much longer than that of cells growing in petri dish (see the supplementary material³⁵ for Figure S4). In particular, encapsulated cells always keep a spherical morphology in contrast to the spindle-like shape of cells cultured in petri dish. During cell division in particles, cells elongate first, followed by the formation of two daughter cells. Notably, newborn daughter cells always stick tightly to their maternal cells and keep their spherical morphology. Occasionally, remerging of newborn daughter cells with their maternal cells is observed (Figure 3(a), (multimedia view)). As a result, the proliferation rate of encapsulated HCT116 cells is much lower than that of HCT116 cells growing in petri dish (Figure 3(b)).

In addition, we notice that when encapsulated HCT116 cells are cultured for 4 days, there are more particles containing 3 cells than that with 2 cells (Figure 3(c)). In particular, when the number of cells at different culture time is evaluated by using $(n_n - n_0)/n_0 \times 100\%$, where n_n is the number of particles containing 2 or 3 cells quantified at day n , ($n=1, 2, 3,$ and 4) and n_0 is

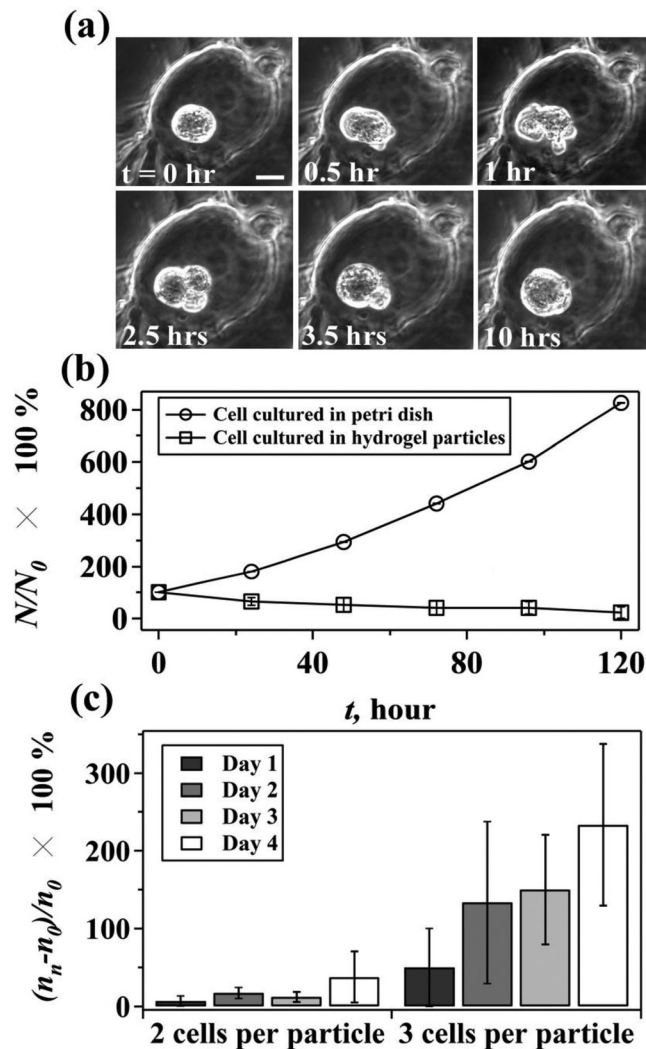


FIG. 3. Proliferation of human HCT116 colon cancer cells in hydrogel particles. (a) Time-series image of the growth of a single cell in a hydrogel particle. Note that at $t = 3.5$ h, daughter cells begin to shrink back into their maternal cell (scale bar = $10 \mu\text{m}$). (b) Percentage of living cells at different time when cells are cultured in petri dish and hydrogel particles. N_0 is the number of living cells at $t = 0$ h, and N is number of living cells at $t = n$ hours ($n = 24, 48, 72, 96,$ and 120). (c) The net growth rate $(n_n - n_0)/n_0 \times 100\%$ of cells encapsulated in hydrogel particles. n_n is the number of particles containing 2 or 3 cells quantified at day n , $n = 1, 2, 3,$ and 4 . n_0 is the number of particles containing 2 or 3 cells collected at day 0. Error bar is presented as standard deviations of the mean. (Multimedia view) [URL: <http://dx.doi.org/10.1063/1.4916508.1>]

the number of particles containing 2 or 3 cells collected at day 0, the percentage of particles containing 3 cells increases dramatically within 4 days. The observation might result from a declined proliferation rate when more cells are encapsulated in one particle. Assuming cells encapsulated in particles with 3 cells stop growing on day 3, for example, there would be more particles containing 3 cells on day 4 because of the high proliferation rate of cells encapsulated in particles with 1 or 2 cells. Thus, accumulation of particles containing 3 cells is expected when the growth rate of cells in particles with 3 cells is lower than that of particles with 1 or 2 cells. Indeed, because encapsulated cells are required to overcome the effect of physical impediments from the matrix and remodel their extracellular microenvironment to create enough space to migrate and proliferate,^{27,28} it is likely that a crowded microenvironment due to increased numbers of cells per particle exerts additional physical confinement that suppresses the proliferation of encapsulated cells. Our results demonstrate, for the first time, the relationships between the number of encapsulated cells and cell proliferation. However, it should be

noted that our results do not exclude the possibility of the influence of cellular communication due to different number of cells.

Last, because chronic inflammation is associated with colon cancer, we further study the dynamic responses of encapsulated colon cancer cells to inflammatory cytokines such as TNF- α (Tumor Necrosis Factor-alpha) (Figure 4).²⁹ TNF- α is a cytokine involved in systematic inflammation and stimulation of acute phase reaction.³⁰ It has been demonstrated previously that TNF- α is able to inhibit the growth of HCT116 cells cultured in petri dish and induces programmed cell death.³¹ In our experiment, where encapsulated human HCT116 cells are treated with different concentrations of TNF- α , the cell viability decreases with the increase of concentration of TNF- α . High concentrations of TNF- α , e.g., above the pathological concentration of TNF- α in colon (5 ng ml^{-1}),³⁰ accelerate cell death (Figure 4(a)), which is similar with the results obtained from cells cultured in petri dish (Figure 4(b)). Cells cultured in petri dish, however, live longer than cells cultured in particles, and can adapt to a low TNF- α concentration, e.g., 0.1 ng ml^{-1} . Cells cultured in particles undergo apoptosis rapidly between 70 and 140 h, depending on the concentration of TNF- α , and do not show the ability to adapt to a low concentration of TNF- α . The observed phenomena may arise from the fact that there is a critical concentration of TNF- α above which cells start to undergo apoptosis.³² When cells are encapsulated in a 3D hydrogel matrix, e.g., Extracel hydrogel particles, however, hydrogel matrix may act as a constrained, stiff network that impairs cell migration and proliferation via regulations of cellular signaling pathways such as integrin ligation, protein kinase activity, and activation of Rho family GTPases,^{27,33,34} and thus leads to a descending cell viability. In this case, the additional stimulation by TNF- α may accelerate cell apoptosis by further activating TNF- α -induced cell apoptosis pathways. However, it should be noted that in the first 24 h cells

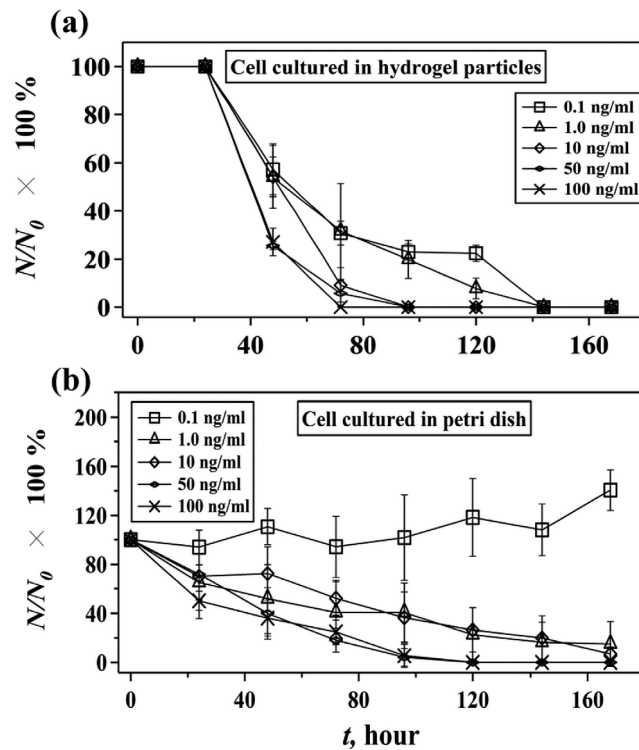


FIG. 4. Effect of TNF- α on the viability of human HCT116 cells cultured in hydrogel particles and petri dish. The change of percentage of living cells, ($N/N_0 \times 100\%$), with time at different concentrations of TNF- α when cells are cultured in hydrogel particles (a) and petri dish (b). N_0 is the number of living cells at $t=0$ h, and N is number of living cells at $t=n$ hours ($n=24, 48, 72, 96, 120, 144, \text{ and } 168$). Error bar is presented as standard deviations of the mean that is calculated based on three sets of independent experiments.

encapsulated in particles have a higher viability than cells cultured in petri dish do. The reason for this phenomenon remains unclear to us. A possible explanation is the slow diffusion rate of TNF- α in hydrogel particles or a gradient of TNF- α across the particle that may delay the effect of TNF- α on cell viability in the early stage of treatment.

CONCLUSIONS

We have demonstrated a microfluidic approach to generate oil-free, cell-containing hydrogel particles by utilizing PFP as the continuous oil phase. Highly efficient removal of PFP by evaporation contributes to a comparably long time, 216 h, culture of encapsulated human HCT116 colon cancer cells. An apparent cell growth in hydrogel particles is observed at both population and single cell levels. When cells are treated with an inflammatory cytokine TNF- α , encapsulated cells are more susceptible to the TNF- α stimuli than cells cultured in petri dish, highlighting the regulatory role of matrix in cancer cells growth under inflammatory conditions. The developed strategy provides an effective approach to obtain cell-containing hydrogel particles without oil contamination and may serve as a potentially useful platform for the development of hydrogel particle-based 3D cell culture, tissue engineering, and cell-based drug delivery.

ACKNOWLEDGMENTS

The authors gratefully acknowledge the support from the Rochester Institute of Technology. We also thank Professor Sindy Tang for help on the amine-modified Krytox.

- ¹G. D. Nicodemus and S. J. Bryant, *Tissue Eng., Part B* **14**, 149 (2008).
- ²H. Liu and K. Roy, *Tissue Eng.* **11**, 319 (2005).
- ³N. T. Elliott and F. Yuan, *J. Pharm. Sci.* **100**, 59 (2011).
- ⁴G. Orive, S. K. Tam, J. L. Pedraz, and J. P. Hallé, *Biomaterials* **27**, 3691 (2006).
- ⁵M. B. Oliveira and J. F. Mano, *Biotechnol. Prog.* **27**, 897 (2011).
- ⁶M. Serra, C. Correia, R. Malpique, C. Brito, J. Jensen, P. Bjorquist, M. J. Carrondo, and P. M. Alves, *PLoS One* **6**, e23212 (2011).
- ⁷A. Murua, M. de Castro, G. Orive, R. M. Hernández, and J. L. Pedraz, *Biomacromolecules* **8**, 3302 (2007).
- ⁸A. Oliveira, T. Moretti, C. Boschini, J. Baliero, L. Freitas, O. Freitas, and C. Favaro-Trindade, *Drying Technol.* **25**, 1687 (2007).
- ⁹T. Kobayashi, Y. Aomatsu, H. Kanehiro, M. Hisanaga, and Y. Nakajima, *Transplant. Proc.* **35**, 484 (2003).
- ¹⁰B. G. Chung, K. Lee, A. Khademhosseini, and S. Lee, *Lab Chip* **12**, 45 (2012).
- ¹¹J. Wan, A. Bick, M. Sullivan, and H. A. Stone, *Adv. Mater.* **20**, 3314 (2008).
- ¹²A. Kumachev, E. Tumarkin, G. C. Walker, and E. Kumacheva, *Soft Matter* **9**, 2959 (2013).
- ¹³T. Kong, L. Wang, H. M. Wyss, and H. C. Shum, *Soft Matter* **10**, 3271 (2014).
- ¹⁴D. E. Morbeck, Z. Khan, D. R. Barnidge, and D. L. Walker, *Fertil. Steril.* **94**, 2747 (2010).
- ¹⁵A. Van Soom, A. Mahmoudzadeh, A. Christophe, M. Ysebaert, and A. De Kruif, *Reprod. Domest. Anim.* **36**, 169 (2001).
- ¹⁶K. Ludwig, E. S. Tse, and J. Y. J. Wang, *BMC Cancer* **13**, 221 (2013).
- ¹⁷C. Buhmann, P. Kraeche, C. Leuders, P. Shayan, A. Goel, and M. Shakibaei, *PLoS One* **9**, e107514 (2014).
- ¹⁸N. Yamamoto, S. Yokoyama, J. Ieda, Y. Mitani, S. Yamaguchi, K. Takifuji, T. Hotta, K. Matsuda, T. Watanabe, J. E. Shively, and H. Yamaue, *Cancer Chemother. Pharmacol.* **75**, 421 (2015).
- ¹⁹S. Guruswamy, M. V. Swamy, C. Choi, V. E. Steele, and C. V. Rao, *Int. J. Cancer* **122**, 25 (2008).
- ²⁰H. Dolznig, C. Rupp, C. Puri, C. Haslinger, N. Schweifer, E. Wieser, D. Kerjaschki, and P. Garin-Chesa, *Am. J. Pathol.* **179**, 487 (2011).
- ²¹A. C. Luca, S. Mersch, R. Deenen, S. Schmidt, I. Messner, K. Schafer, S. E. Baldus, W. Huckenbeck, R. P. Piekorz, W. T. Knoefel, A. Krieg, and N. H. Stoecklein, *PLoS One* **8**, e59689 (2013).
- ²²G. Yang, H. Zhang, and G. D. Prestwich, *J. Can. Res. Updates.* **1**, 69 (2012).
- ²³C. Holtze, A. Rowat, J. Agresti, J. Hutchison, F. Angile, C. Schmitz, S. Köster, H. Duan, K. Humphry, and R. Scanga, *Lab Chip* **8**, 1632 (2008).
- ²⁴E. Tumarkin, L. Tzadu, E. Csazar, M. Seo, H. Zhang, A. Lee, R. Peerani, K. Purpura, P. W. Zandstra, and E. Kumacheva, *Integr. Biol.* **3**, 653 (2011).
- ²⁵A. Kumachev, J. Greener, E. Tumarkin, E. Eiser, P. W. Zandstra, and E. Kumacheva, *Biomaterials* **32**, 1477 (2011).
- ²⁶A. R. Abate, T. Hung, P. Mary, J. J. Agresti, and D. A. Weitz, *Proc. Natl. Acad. Sci.* **107**, 19163 (2010).
- ²⁷J. A. Green and K. M. Yamada, *Adv. Drug Deliv. Rev.* **59**, 1293 (2007).
- ²⁸G. Raeber, M. Lutolf, and J. Hubbell, *Acta Biomater.* **3**, 615 (2007).
- ²⁹D. C. Rubin, A. Shaker, and M. S. Levin, *Front. Immunol.* **3**, 107 (2012).
- ³⁰S. F. van Eeden, W. C. Tan, T. Suwa, H. Mukae, T. Terashima, T. Fujii, D. Qui, R. Vincent, and J. C. Hogg, *Am. J. Respir. Crit. Care Med.* **164**, 826 (2001).

- ³¹P. Wang, W. Qiu, C. Dudgeon, H. Liu, C. Huang, G. Zambetti, J. Yu, and L. Zhang, *Cell Death Differ.* **16**, 1192 (2009).
- ³²D. A. Turner, P. Paszek, D. J. Woodcock, D. E. Nelson, C. A. Horton, Y. Wang, D. G. Spiller, D. A. Rand, M. R. White, and C. V. Harper, *J. Cell Sci.* **123**, 2834 (2010).
- ³³L. G. Griffith and M. A. Swartz, *Nat. Rev. Mol. Cell Biol.* **7**, 211 (2006).
- ³⁴K. M. Yamada and E. Cukierman, *Cell* **130**, 601 (2007).
- ³⁵See supplementary material at <http://dx.doi.org/10.1063/1.4916508> for cell culture and maintenance, microfluidic generation of droplets and microparticles with encapsulated HCT116 cells, and calculation for number of cells in drops. In Figure S1, we show theoretical Poisson distribution of cells in drops. Figure S2 claims evaporation-induced change of weight percentage of the mixture solution of droplets and HFE 7500 oil. In Figure S3, we show the separation of the oil phase from particles by using conventional approaches such as centrifugation and filtration. Figure S4 indicates proliferation rate of HCT116 cells cultured in petri dish.